Exploring the relationship of *Homalosilpha* and *Mimosilpha* (Blattodea, Blattidae, Blattinae) from a morphological and molecular perspective, including a description of four new species

Shuran Liao, Yishu Wang, Duting Jin, Rong Chen, Zongqing Wang and Yanli Che

College of Plant Protection, Southwest University, Chongqing, Beibei, China

ABSTRACT

This study utilized six genes (*12S*, *16S*, *18S*, *28S*, *COII* and *H3*) from a total of 40 samples to construct maximum likelihood (ML) and Bayesian inference (BI) phylogenetic trees in order to infer the relationships between the morphologically similar genera *Homalosilpha* Stål, 1874 and *Mimosilpha* Bey-Bienko, 1957. The phylogenetic analysis showed the two genera have a close relationship and were recovered as sister groups based on ML and BI analyses. Four new species are described among these samples, i.e., *Homalosilpha obtusangula* sp. nov., *Homalosilpha recta* sp. nov., *Homalosilpha alba* sp. nov. and *Homalosilpha clavellata* sp. nov. based on morphological and *COI* data. A key to the worldwide *Homalosilpha* is provided.

INTRODUCTION

Genus *Homalosilpha* Stål, 1874 is remarkable in the family of Blattidae for its flat pronotum decorated with black or white markings (*Princis, 1966a*; *Roth, 1999*). *Stål (1874)* established *Homalosilpha* with *Periplaneta ustulata* Burmeister, 1838 as the type species. Then *Kirby (1904)* transferred three *Periplaneta* Burmeister, 1838 species to *Homalosilpha*. *Homalosilpha* can be easily distinguished from *Periplaneta* by the discoidal pronotum whose surface is scattered with various spots, sides are not deflexed and with greatest width at the middle (*Shelford, 1910*). Subsequently, two species were reported from Uganda and China by *Shelford (1908)*, *Shelford (1910)*. Later, *Princis (1966a)* described two species from Congo and Indonesia and provided a key for eight *Homalosilpha* species. In 1969, Bey-Bienko described four species, of which three species were from China. *Kumar (1975)* synonymized *H. vicina* Brunner von Wattenwyl, 1865 with *H. cruralis* Shelford, 1908 because the diagnostic characters used, the color of the tibiae and the anterior and posterior margin of pronotum, were variable and should be treated as intraspecific variation. After the examination of specimens from Malaysia and Indonesia by *Roth (1999)*, *Homalosilpha quadrimaculata* was described on the basis of the distinct orange spots on

Corresponding author
Yanli Che, shirleyche2000@126.com

the pronotum. Up to now, a total of twelve species of *Homalosilpha* had been reported worldwide (*Beccaloni, 2014*), of which, *H. arcifera Bey-Bienko, 1969*, *H. gaudens Shelford, 1910*, *H. kryzhanovskii Bey-Bienko, 1969*, *H. ustulata* (*Burmeister, 1838*), and *H. valida Bey-Bienko, 1969* are distributed in China. Without professional taxonomic knowledge about Blattodea, it is challenging to identify the *Homalosilpha* species owing to their high similarity in appearance (Liao SR & Che YL, pers. obs., 2018–2019). Therefore, simple and accurate methods are needed to help the identification of *Homalosilpha* species.

Genus *Mimosilpha* was established with *M. disticha* as type species from Yunnan, China. It is strongly similar to *Homalosilpha* in appearance (*Bey-Bienko, 1957*). The main difference between *Mimosilpha* and *Homalosilpha* is that there are three rows of spines along the edge of the hind tibiae of *Homalosilpha*, while *Mimosilpha* only has two rows of spines. Only one *Mimosilpha* species has been recorded in the world (*Beccaloni, 2014*).

DNA barcodes proved to be an effective tool to aid the identification of the similar species and even resolve the problem of sexual dimorphism in cockroaches (*Evangelista, Buss & Ware, 2013*; *Che et al., 2017*; *Liao, Wang & Che, 2019*). Multi-gene combination phylogenetic trees are increasingly applied in cockroach systematics to explore the problem of paraphyly (*Inward, Beccaloni & Eggleton, 2007*; *Ware et al., 2008*; *Legendre et al., 2015*), establish new taxa (*Evangelista et al., 2019*), infer possible sister group (*Djernæs, Klass & Eggleton, 2015*; *Wang et al., 2017*), and then revise the taxonomy (*Djernæs, 2018*). These studies have all been demonstrated to be informative and successful in revealing relationships among different groups via multi-gene analysis. *Mimosilpha* and *Homalosilpha* are very close in morphology with a confused taxonomy, so it is urgent to sequence six genes to infer the relationship of these two genera.

In this study, 13 COI sequences of *Homalosilpha* and *Mimosilpha* species were obtained in order to help distinguish species when combined with morphological data. We also sequenced three mitochondrial genes (*12S*, *16S* and *COII*) and three nuclear genes (*18S*, *28S* and *H3*) to explore the phylogenetic relationship of *Homalosilpha* and *Mimosilpha*. Moreover, we illustrate four new *Homalosilpha* species from China based on morphological characters and DNA barcoding.

MATERIALS AND METHODS

Morphological study

Morphological terminology used in this paper mainly follows *McKittrick (1964)*, *Roth (2003)* and *Li et al. (2018)*.

The maculae on the pronotum provided effective information for the identification of *Homalosilpha* species, which could be grouped into three types (*Shelford, 1910*; *Princis, 1966a*; *Bey-Bienko, 1969*; *Roth, 1999*): (1) white spots scattered on the black pronotum, represented by *H. decorata* and *H. quadrimaculata*, (2) one large central dark spot on the pale brown pronotum, represented by *H. hanni*, *H. nigricans* and *H. gaudens*, and (3) the symmetrical multiple spots and stripes on the disk of the pale brown pronotum, represented by the remaining *Homalosilpha* species. The third type is more complex than the former two, so we herein address the specific part of the maculae for description as shown in Fig. 1.
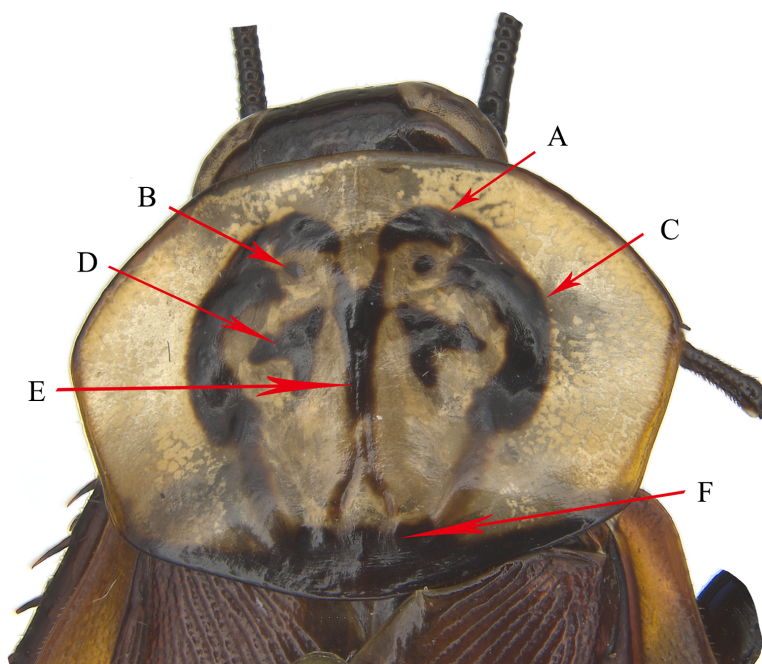
Figure 1 **The pronotum of *H. obtusangula* sp. nov.** (A) Anterior pattern. (B) Small spot. (C) Lateral pattern. (D) Central pattern. (E) Vertical pattern. (F) Posterior band. Scale bars = 5 mm.

All specimens were measured by vernier caliper for the body length from the anterior to the posterior, for the body length including tegmina from the anterior to the tip of tegmina, and pronotum length × width at the longest and the widest part. Genital segments of the examined specimens were macerated and photographs (Figs. 1–9) of the specimens were taken as previously described in *Liao, Wang & Che (2019)*. The type materials are deposited in the Institute of Entomology, College of Plant Protection, Southwest University, Chongqing, China (SWU).

DNA extraction, PCR, and sequencing

We sampled seven genes of 13 species (Tables S1 and S2) from *Homalosilpha* in this study: mitochondrial *12S*, *16S*, cytochrome *c* oxidase subunit I (*COI*) and subunit II (*COII*), and nuclear *18S*, *28S*, and histone *H3*. Total DNA was extracted from the leg tissue of samples according to the Hipure Tissue DNA Mini Kit (Tsingke Biological Technology, Beijing, China). All fragments were amplified using PCR; primers for amplifications are given in Table 1. Reactions were carried out in volumes of 25 μL, containing 22 μL of 1 × 1 T3 supper mix (Tsingke Biological Technology, Beijing, China), 1 μL of each primer and 1 μL of DNA template, except for COII containing 12.5 μL T2 mix (Tsingke Biological Technology, Beijing, China), 8.5 μL of ultrapure water, 1 μL of each primer and 2 μL of DNA template. The amplification conditions were: initial denaturation at 98 °C for 2 min, followed by 35 cycles for 10 s at 98 °C, 10 s at 43−55 °C, and 15 s at 72 °C, with a final extension of 2 min at 72 °C; however for COII: initial denaturation at 94 °C for 5 min,
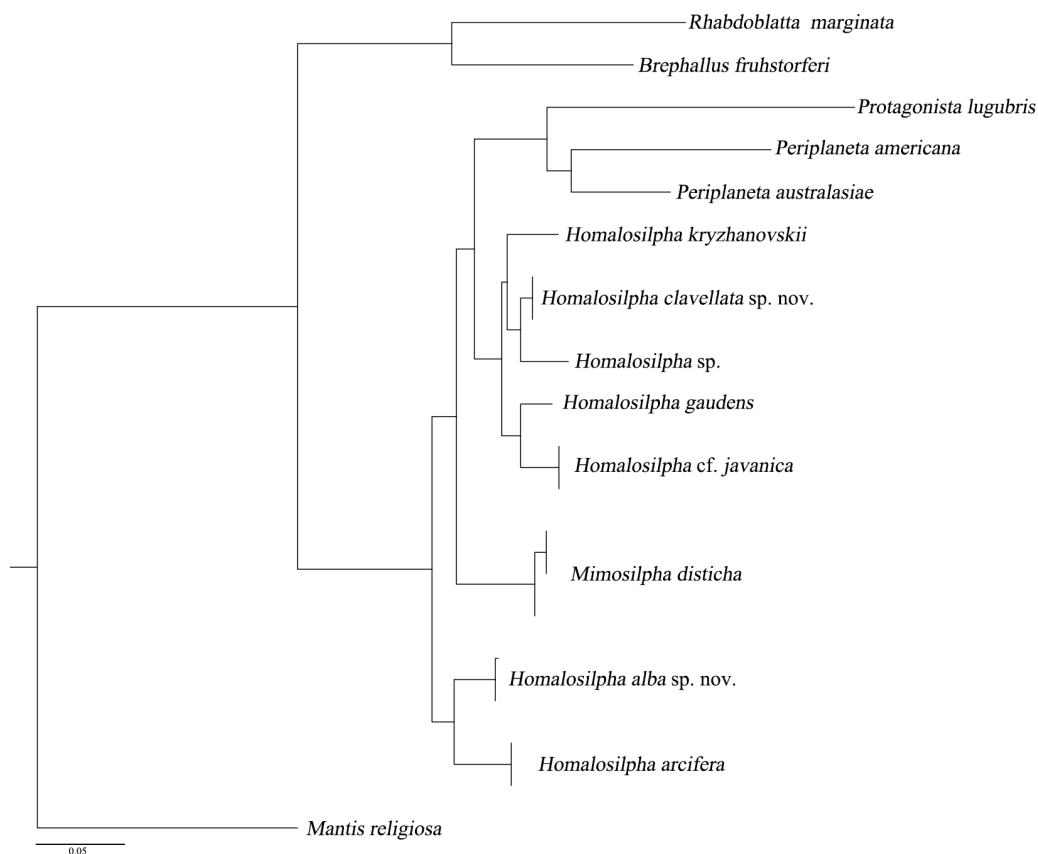
Figure 2 **Maximum likelihood (ML) tree of the cockroaches based on *COI*.** ML tree derived from COI gene analysis following GTRGAMMA model with 1,000 bootstrap replicates.

followed by 35 cycles for 45 s at 94 °C, 45 s at 50 °C, and 45 s at 72 °C, with a final extension of 10 min at 72 °C. All sequences were deposited in GenBank (accession numbers in Tables S1 and S2).

Sequence processing and phylogenetic analyses

In this study, a total of 14 *COI* sequences, whose lengths were 658 bp, were combined with one *Protagonista*, two *Periplaneta*, one *Rhabdoblatta*, one *Brephallus* and one mantid sequence to infer species delimitation analysis for *Homalosilpha* and *Mimosilpha* (Table S1). Intraspecific and interspecific genetic divergence values are quantified based on the Kimura 2-parameter (K2P) distance model (*Kimura, 1980*), using MEGA 7 (*Kumar, Stecher & Tamura, 2016*).

To infer the relationship of *Homalosilpha* and *Mimosilpha*, we included sequence data from 22 Blattidae taxa (ingroup including seven *Homalosilpha* and one *Mimosilpha* species) and 12 outgroup taxa (Table S2). These analyses were performed based on six genes (*12S*, *16S*, *18S*, *28S*, *COII* and *H3*). These data was aligned by online Mafft 7 (https://mafft.cbrc.jp/alignment/server/), and the methods were the same as *Wang et al. (2017)*. Specifically, the Q-INS-i algorithm was selected for non-coding protein genes (*12S*,

16S, *18S*, *28S*), the G-INS-i algorithm was selected for coding protein genes (*COII*, *H3*) and used with other parameters at their default values. Alignments of sequences were inspected visually and manually adjusted in MEGA 7.0. Poorly aligned characters were removed but these were limited. The remaining bases are as following: 424nt for *12S*, 447nt for *16S*, 1814nt for *18S*, 596nt for *28S*, 665nt for *COII*, 328nt for *H3*.

The molecular data set was divided into eight partitions (partitioned by gene: *12S*, *16S*, *18S*, *28S*, *COII*_pos1, *COII*_pos2, *H3*_pos1, and *H3* _pos2). We excluded the third codon positions of the protein-coding genes (*COII* and *H3*) because of the high level of mutational saturation. The third codon position (pos3) ($I_{SS} = 0.977$) was much more saturated than the first and second codon position (pos12) ($I_{SS} = 0.493$) after using Xia's method implemented in DAMBE 5.0 (*Xia, 2013*). Phylogenetic analyses were constructed using maximum likelihood (ML) and Bayesian inference methods. ML analyses were performed using RaxML 7.7.1 (*Stamatakis, Hoover & Rougemont, 2008*), and BI analyses were performed using MrBayes 3.2 (*Ronquist et al., 2012*). ML analyses was performed using RAxML v.7.7.1 (*Stamatakis, Hoover & Rougemont, 2008*). We used the GTRGAMMA model for the combined datasets with 1,000 bootstrap replicates. For BI analyses, PartitionFinder v.1.1.1 (*Lanfear et al., 2012*) was utilized to choose models and model selection was based on BIC. For eight partitions, the best-fitting substitution models are as follows: GTR+I+G: *12S*, *16S*; TIMef+I+G: *18S*, *H3*_pos1, *H3*_pos 2; TrN+I+G: *28S*, *COII*_pos1, *COII*_pos2. Two independent sets of Markov chains were run, each with one cold and three heated chains for 5,000,000 generations, and every 1,000th generation was sampled. Convergence was inferred when a standard deviation of split frequencies < 0.01 was completed. The ESS values are all more than 200.

RESULTS

Species delimitation based on *COI* and morphological data

In this study, we acquired 14 *COI* sequences representing seven *Homalosilpha* and 1 *Mimosilpha* species. All of the new sequences have been deposited in GenBank with accession numbers MW201581–MW201594 (Table S1). The *COI* sequences we acquired had a relatively high AT content (67.2%), with an average nucleotide composition of A = 31%, T = 36.2%, C = 16.5%, and G = 16.3%. Sequence analysis revealed that 109 (16.57%) sites were variable, of which 79 (12%) sites were parsimoniously informative. ML analysis revealed that clades from the same species, constituted monophyletic groups with high support values (Fig. 2). In particular, the male and female of *H. clavellata* sp. nov., which have different markings on the pronotum, could be matched by COI data.

We observed the lowest and largest K2P interspecies genetic distance (Table 2) among these species. The lowest distance 0.031 was between *Homalosilpha* sp. and *H. clavellata* sp. nov., the largest distance 0.084 between *H. nigricans* and *H. arcifera*, *H. arcifera* and *H. kryzhanovskii,* as well as *M. disticha* and *H. kryzhanovskii*. Morphologically, although having a low genetic distance, *Homalosilpha* sp. and *H. clavellata* sp. nov. show distinct differences in the maculae on the pronotum, the band in the interocular space (*H. clavellata* sp. nov.: yellow and straight transverse band, *Homalosilpha* sp.: yellow and tortuous transverse
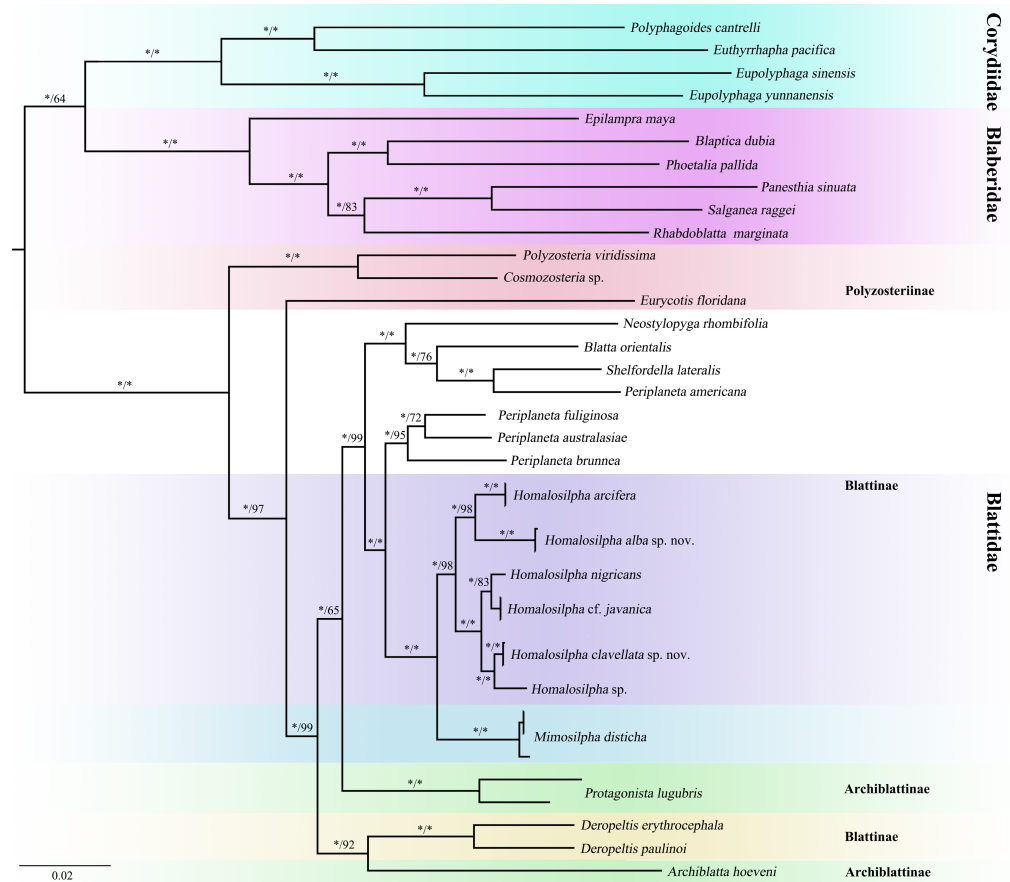
Figure 3 Maximum likelihood (ML) tree of the cockroaches based on six genes. ML tree derived from analysis of combined data *12S*, *16S*, *18S*, *28S*, *COII*, and *H3* genes. Branch labels are support for our analyses in the following order: bootstrap supports of the maximum-likelihood tree, Bayesian posterior probabilities of the Bayesian tree; asterisks (*) indicate 100% support for a given analysis. The topology shown was totally similar to that derived from BI analysis.

band) and even in the female genitalia (*H. clavellata*: anterior of basivalvula with spots, the shape of first valvule uniform, *Homalosilpha* sp.: surface of basivalvula with fold, the end of the first valvula swollen). Finally, a total of 8 *Homalosilpha* and *Mimosilpha* species were recovered after combining the results of molecular data with morphological data, of which 4 species are new to science: *H. obtusangula* sp. nov., *H. recta* sp. nov., *H. alba* sp. nov., and *H. clavellata* sp. nov. More details about these new *Homalosilpha* species are provided below.

Relationship of *Homalosilpha* and *Mimosilpha* inferred from two phylogenetic analyses

We acquired 12 *12S*, 12 *16S*, 11 *18S*, 12 *28S*, 10 *COII*, 12 *H3* sequences with accession numbers MW218556–MW218578, MW219581–MW218604 and MW201809–MW201830 (Table S2). For the concatenate dataset (*12S*, *16S*, *18S*, *28S*, *COII*, *H3*), our likelihood and Bayesian phylogenetic analyses yielded totally identical topologies with generally
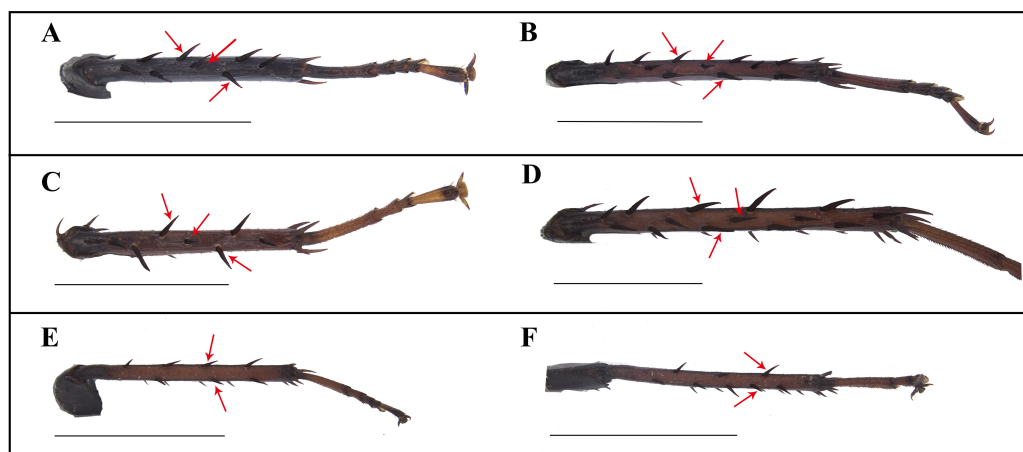
Figure 4 Photographs of middle and hind tibiae of *Homalosilpha* and *Mimosilpha* species. (A–B) *H. nigricans* Princis, 1966a. (C–D) *H. alba* sp. nov. (E–F) *M. disticha.* Middle and hind tibiae are seen on dorsal view. Scale bars = 5 mm.

high node support (Fig. 3 and Fig. S1). All genera of Blattidae clustered together and formed a highly supported monophyletic group (MLB = 100, BPP = 100). Five recognized major lineages of Blattidae from ML and BI inferences were recovered, represented by members of Polyzosteriinae, Archiblattinae and Blattinae. According to our inferred trees, Polyzosteriinae, Archiblattinae and Blattinae were paraphyletic with high support values.

The topology derived from ML and BI analyses shows that all *Homalosilpha* members cluster together and are recovered as the sister group of *Mimosilpha* (MLB = 100, BPP = 100). *H. clavellata* sp. nov. and *Homalosilpha* sp. were recovered as sister groups with strong support values, which is consistent with the inference based on *COI* data. And the result is same as the trees of seven genes (*12S, 16S, 18S, 28S, COI, COII, H3*) (Figs. S2 and S3).

The electronic version of this article in Portable Document Format (PDF) will represent a published work according to the International Commission on Zoological Nomenclature (ICZN), and hence the new names contained in the electronic version are effectively published under that Code from the electronic edition alone. This published work and the nomenclatural acts it contains have been registered in ZooBank, the online registration system for the ICZN. The ZooBank LSIDs (Life Science Identifiers) can be resolved and the associated information viewed through any standard web browser by appending the LSID to the prefix http://zoobank.org/. The LSID for this publication is: [74F6BF88-9FFD-40DB-9C8B-D7650491F0EE]. The online version of this work is archived and available from the following digital repositories: PeerJ, PubMed Central and CLOCKSS.

Taxonomy

Homalosilpha Stål, 1874

Homalosilpha Stål, 1874: 13. Type species: *Homalosilpha ustulata Burmeister, 1838*. *Kirby, 1904*: 143; *Shelford, 1910*: 19; *Hanitsch, 1915*: 112; *Princis, 1966a*: 49; *Princis, 1966b*: 457; *Roth, 1999*: 172.

Diagnosis. Body medium to large, flat, smooth, generally brownish to blackish. Antennae long, slender. Pronotum flat, decorated with maculae, sides not deflexed, greatest width near the middle. Tegmina and wings extending considerably beyond the apex of the abdominal tip. Legs long, front femora Type A_2, the outer edge of the middle and hind tibiae each with three rows of spines (Fig. 4); tarsal claws simple, symmetrical. Supra-anal plate broad. Cerci long. Subgenital asymmetrical. Male genitalia: left and right phallomere all consisting of three parts. L1 fold sclerite; margin of L2d with serration; posterior of L2v produced with a spiny projection to the end; L3 unciform, the terminal bifurcate. R1 foot-shaped, left margin with two spines; terminal of R2d projected, R2v folded sclerite; R3 broad and folded sclerite. In the nymph, the body shows zebra-like stripes.

Checklist of *Homalosilpha* worldwide

Homalosilpha alba sp. nov. China
Homalosilpha arcifera Bey-Bienko, 1969 China, Vietnam
Homalosilpha contraria (Walker, 1868) Philippines
Homalosilpha decorata (Serville, 1838) Indonesia (Sumatra), Indonesia (Java Island), Borneo Island
Homalosilpha gaudens Shelford, 1910 China, Vietnam
Homalosilpha haani Princis, 1966a Indonesia
Homalosilpha clavellata sp. nov. China
Homalosilpha javanica Bey-Bienko, 1969 Indonesia
Homalosilpha kryzhanovskii Bey-Bienko, 1969 China
Homalosilpha nigricans Princis, 1966 Congo Democratic Republic
Homalosilpha obtusangula sp. nov. China
Homalosilpha recta sp. nov. China
Homalosilpha quadrimaculata Roth, 1999 Malaysia
Homalosilpha ustulata (*Burmeister, 1838*) China, Myanmar, Malaysia, Indonesia, Philippines
Homalosilpha valida Bey-Bienko, 1969 China
Homalosilpha vicina (*Brunner von Wattenwyl, 1865*) Guinea, Cameroon, Uganda
Homalosilpha sp. China

Key to *Homalosilpha* species worldwide

1. Pronotum mostly black …2
Pronotum mostly white…3
2. Pronotum with two vertical white stripes near the lateral margin …*H. decorata*
Pronotum with four white spots respectively at the anterior margin and middle…*H. quadrimaculata*
3. Pronotum with a large black spot at center …4

Pronotum with multiple black spots or stripes … 6

4. The large spot connecting both the front and hind margins … *H. haani*

The large spot only connected with the hind margin … 5

5. Pronotum broadest near the hind margin, trapeziform … *H. nigricans*

Pronotum broadest near the middle … *H. gaudens*

6. Face pale yellow … *H. arcifera*

Face black … 7

7. Vertex yellow to yellowish brown … 8

Vertex black … 10

8. Abdomen with yellow spots … *H. valida*

Abdomen brownish black to dark … 9

9. The hind margin of supra-anal plate slightly concave, lateral angles blunt … *H. recta* sp. nov.

The hind margin of supra-anal plate round, lateral angles sharp … *H. alba* sp. nov.

10. Interocular space with a yellow straight band … 11

Interocular space with a yellow band … *H. ustulata*

11. The lateral pattern and vertical pattern of pronotum connected with posterior band, spots on both sides of the lateral pattern … *H. vicina*

The middle of pronotum with spots or spots and stripes, the both sides of lateral pattern without spots… 12

12. Pronotum without vertical pattern … *H. contraria*

Pronotum with vertical pattern … 13

13. The vertical pattern of pronotum with one stripe … 14

The vertical pattern of pronotum with spots … 16

14. The vertical pattern with one short and bold stripe … *H. clavellata* sp. nov.

The vertical pattern with one long stripe and posterior vertical pattern bifurcated … 15

15. The vertical pattern with pinstripe and the anterior pattern connected with lateral pattern … *H. obtusangula* sp. nov.

The vertical pattern with black stripe and the central pattern connected with vertical pattern … *Homalosilpha* sp.

16. The hind margin of supra-anal plate with two sharp valves … *H. javanica*

The hind margin of supra-anal plate with two round valves … *H. kryzhanovskii*

Homalosilpha obtusangula Liao et Che sp. nov.
(Figs. 5A–5D, 7A and 7B, 8A–8C)
urn:lsid:zoobank.org:act:8713E5A8-D25B-4DFB-9E44-3B1E719AE2FC

Holotype. CHINA: Tibet: male (SWUB125-H) Beibeng Township, Mêdog County, 2013.VII.31, Xinglong Bai & Junsheng Shan leg.

Paratype. 1 female (SWUB125-P1), CHINA: Yunnan: Mt. Fenshuiling, Jinping County, 2016.V, Tianlong He leg.

Etymology. The species epithet comes from the Latin word *obtusangulus* in reference to the lateral angles of supra-anal plate being obtuse.

Description. Male. Body length 24.4 mm; overall length including tegmen 33.8 mm; pronotum length × width 6.4 × 8.4 mm. Female. Body length 26.5 mm; overall length including tegmen 36.3 mm; pronotum length × width 6.8 × 8.9 mm.

Coloration. Similar in both sexes. Body generally dark brown (Figs. 5A and 5B). Interocular space with a whitish transverse band. Pronotum white, margins black outlined, hind margin black; center of the pronotum with symmetrical blackish markings (Figs. 5C and 5D). Tegmen reddish brown, wing hyaline, brownish except the anal area (Figs. 7A and 7B). Tibiae and tarsi dark reddish brown (Fig. 5B).

Head with vertex unsheltered by pronotum. Interocular distance slightly narrower than the distance between antennae sockets. Pronotum nearly heptagonal, broadest near the middle; the middle of pronotum with black and symmetrical patterns, the anterior pattern connected with lateral pattern, the lateral pattern arc-shaped, central pattern dart-like, the posterior of vertical pattern bifurcated, the posterior band bold (Figs. 5C and 5D). Male supra-anal plate broad and symmetrical, nearly trapezoidal, but with a deep, obtuse-angled invagination at the middle of hind margin; male subgenital plate asymmetrical, left hind corner more protruded than on the right, styli similar, long (Figs. 8A and 8B).

Male genitalia. Left phallomere: L1 fold sclerite; margin of L2d with small serration, posterior of L2v produced as a spiny projection to the end; L3 unciform, the base broad, tapering down, the terminal bifurcate, one branch short, the other long (Fig. 8C). Right phallomere: R1 foot-shaped, left margin with two spines; terminal of R2d sharp, R2v fold sclerite; R3 broad and fold sclerite (Fig. 8C).

Remarks. *H . obtusangula* sp. nov. resemble *H. kryzhanovskii*, but can be distinguished from *H. kryzhanovskii* by the following characters: (1) the pronotum with stripes in the former, while the latter with spots; (2) the hind margin of supra-anal plate deeply concave, while the latter, hind margin slightly concave; (3) the lateral corner sharp in the former, while the latter, the lateral corner rounded

Homalosilpha recta Liao et Che sp. nov.
(Figs. 5E–5H, 7C and 7D, 8D–8F)
urn:lsid:zoobank.org:act:88B30874-14A8-4035-B200-262CF60E09D6

Holotype. CHINA: Yunnan: male (SWUB126-H) Banhong Township, Cangyuan County, 1130 m, 2008.VII.16-18, Jishan Xu & Zhenhua Gao leg.

Etymology. The species epithet '*rectus*' refers to the hind margin of supra-anal plate and subgenital plate being straight.

Description. Male. Body length 28.3 mm; overall length including tegmen 39.9 mm; pronotum length × width 7.3 × 10.6 mm.

Coloration. Body generally dark brown (Figs. 5E and 5F). Vertex and the area between eyes and ocelli white. Pronotum white, subhyaline, with black outline weak, hind margin blackish weakly, middle of the pronotum with sparse, symmetrical blackish markings (Figs.

5G and 5H). Tegmina yellowish brown, wings hyaline, dark brownish except the anal area (Figs. 7C and 7D). Tibiae and tarsi dark reddish brown.

Head with vertex unsheltered by pronotum. Interocular distance narrower than distance between antennae sockets. Pronotum nearly hexagonal, anterior and hind margins slightly outward, broadest near the middle; the anterior pattern triangular, the lateral pattern and central pattern with two parts, the vertical pattern with only one spot, the posterior band indistinct (Figs. 5E and 5F). Male supra-anal plate broad and symmetrical, nearly trapezoidal, with a very shallow, obtuse-angled invagination at the middle of hind margin, hind lateral angles slightly protruded laterally; subgenital plate of male asymmetrical, quadrate, right lateral hind corner narrowed, styli similar, long (Figs. 8D and 8E).

Male genitalia. Left phallomere: L1 fold sclerite; posterior margin of L2d with small spines, posterior of L2v produced as a spiny projection to the end; L3 unciform, the base broad, tapering down, the terminus bifurcate (Fig. 8F). Right phallomere: R1 foot-shaped, left margin with two unequal spines, the spine on the top longer than the bottom; terminal of R2d unciform, R2v fold sclerite; R3 broad (Fig. 8F).

Remarks. *H. recta* sp. nov. is similar to *H. kryzhanovskii* (Figs. 6I–6L, 8M–8O) and *H. alba* sp. nov. (Figs. 5I–5L, 8G–8I), but can be distinguished from *H. kryzhanovskii* by the following characters: (1) the composition of black spots in pronotum; (2) vertex white, while in *H. kryzhanovskii* black; and (3) the hind margin of supra-anal plate slightly concave and with lateral sides curving laterally, however in *H. kryzhanovskii* the two hind angles nearly round. Furthermore, it can be distinguished from *H. alba* sp. nov. by the following characters: (1) the composition of black spots with slight difference; and (2) the hind margin of the supra-anal plate slightly concave and blunt, however in *H. alba*, the lateral angles of the supra-anal plate are sharp.

Homalosilpha alba Liao et Che sp. nov.
(Figs. 5I–5L, 7E and 7F, 8G–8I)
urn:lsid:zoobank.org:act:ED3EEF8E-FD76-47F7-AA5A-ABE9F3CA6724

Holotype. CHINA: Hainan: male (SWUB127-H) Yajiang Scenery Spot, Mt Bawangling, Cangjiang County, 1130 m, 2015.IV.30, Lu Qiu & Qikun Bai leg.
Paratypes. China: Hainan: 1 female (SWUB127-P1). Maogan Township, Baoting County, 2015.IV.11-12, Lu Qiu & Qi-kun Bai leg; 1 female (SWUB127-P2). Mt Diaoluoshan, Lingshui County, 1964.III.28, Si-Kong Liu; 1 female (SWU) Ledong County, 1954.V.4, Keren Huang leg.
Etymology. The species epithet is derived from the Latin word '*albus*', referring to the vertex being white.
Description. Male. Body length 27.2 mm; overall length including tegmen 33.1 mm; pronotum length × width 6.1 × 8.5 mm. Female. Body length 28.3 mm; overall length including tegmen 36.4 mm; pronotum length × width 7 × 9.9 mm.
Coloration: Similar in both sexes. Body dark brown (Figs. 5I and 5J). Vertex and the area between eyes and ocelli white. Pronotum white, margins black outlined, hind margin black
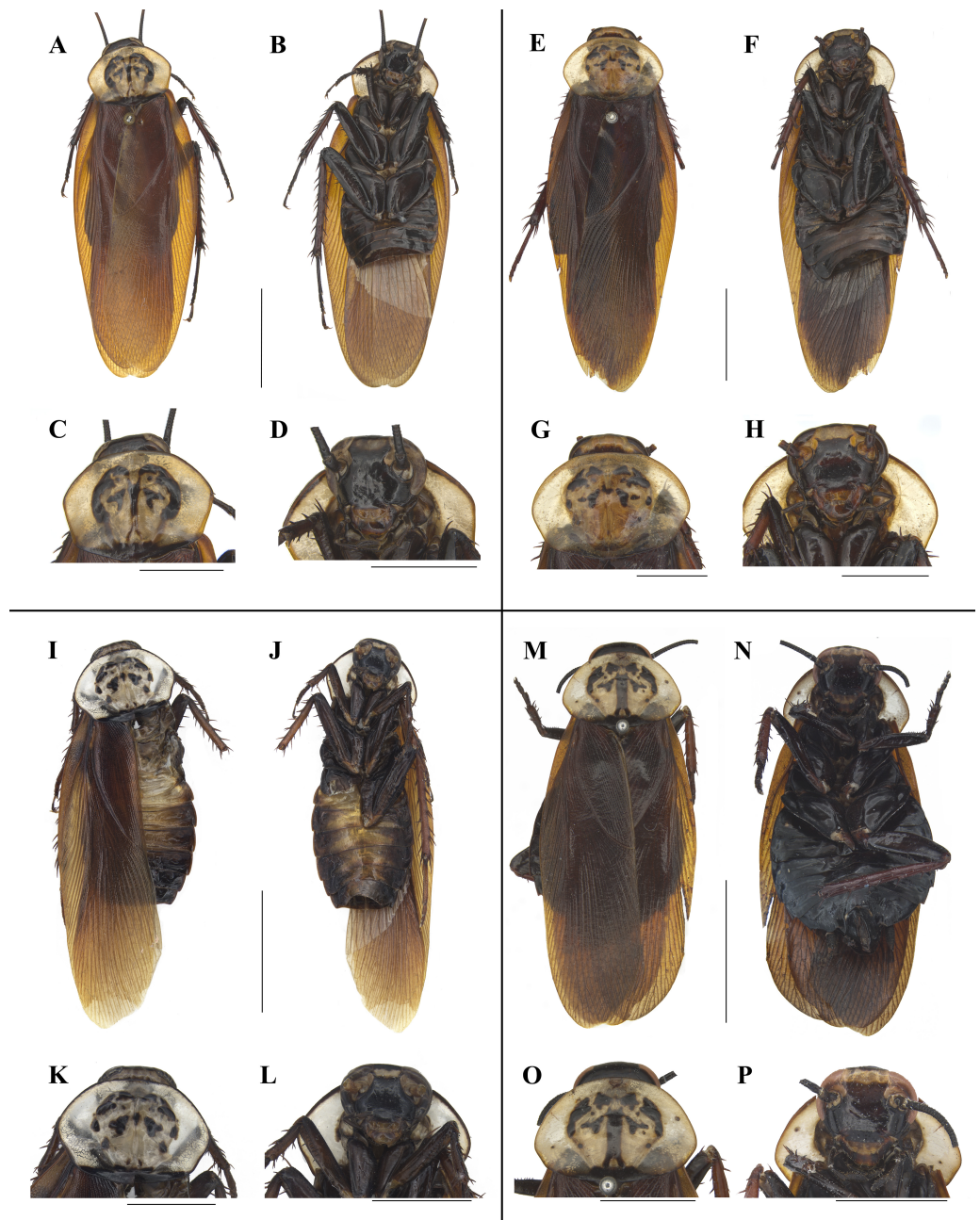
Figure 5 Photographs of bodies, pronotums and faces of four species of *Homalosilpha*. (A–D) *H. obtusangula* sp. nov., male holotype. (E–H) *H. recta* sp. nov., male holotype. (I–L) *H. alba* sp. nov., male holotype. (M–P) *Homalosilpha* sp., female. Scale bars = 10 mm (A, B, E, F, I, J, M, N); 5 mm (C, D, G, H, K, L, O, P).

(Figs. 5K and 5L). Tegmina reddish brown, wings hyaline, brown except the anal area (Figs. 7E and 7F). Middle of the abdomen yellowish brown. Tibiae and tarsi reddish brown (Fig. 5L).
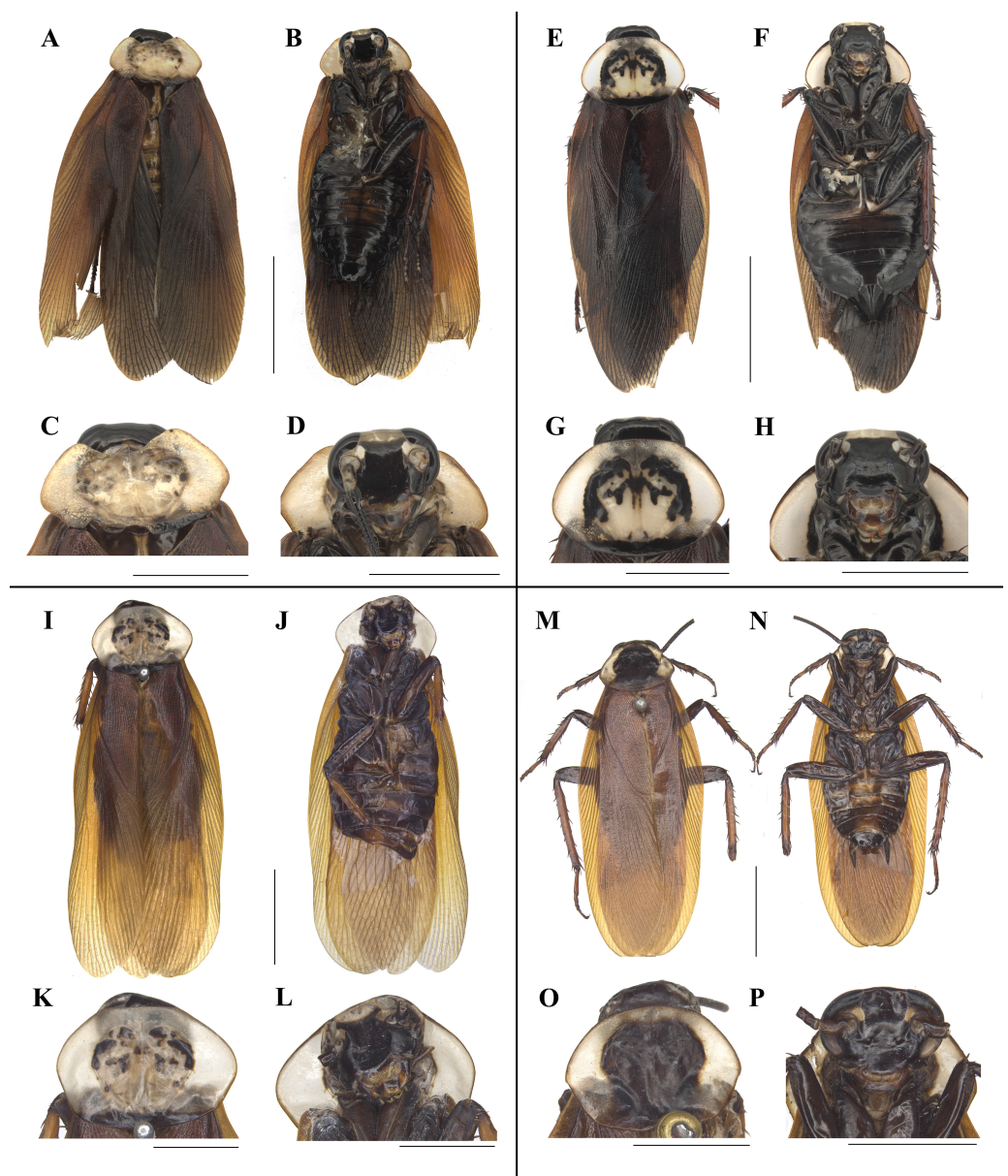
Figure 6 Photographs of bodies, pronotums and faces of two species of *Homalosilpha* and one species of *Mimosilpha*. (A–D) *H. clavellata* sp. nov., male holotype. (E–H) *H. clavellata* sp. nov., female paratype. (I–L) *H. kryzhanovskii*. (M–P) *M. disticha*. Scale bars = 10 mm (A, B, E, F, I, J, M, N); 5 mm (C, D, G, H, K, L, O, P).

Head with vertex unsheltered by pronotum. Interocular distance narrower than the distance between antennae sockets. Pronotum nearly a hexagon, anterior and hind margins slightly outward, broadest near the middle; the anterior pattern and central pattern triangular, the lateral pattern with three parts, the vertical pattern with only one spot, the posterior band bold and with two spots on the band (Fig. 5K). Male supra-anal plate symmetrical, nearly trapezoidal, hind margin widely concave, lateral hind angles
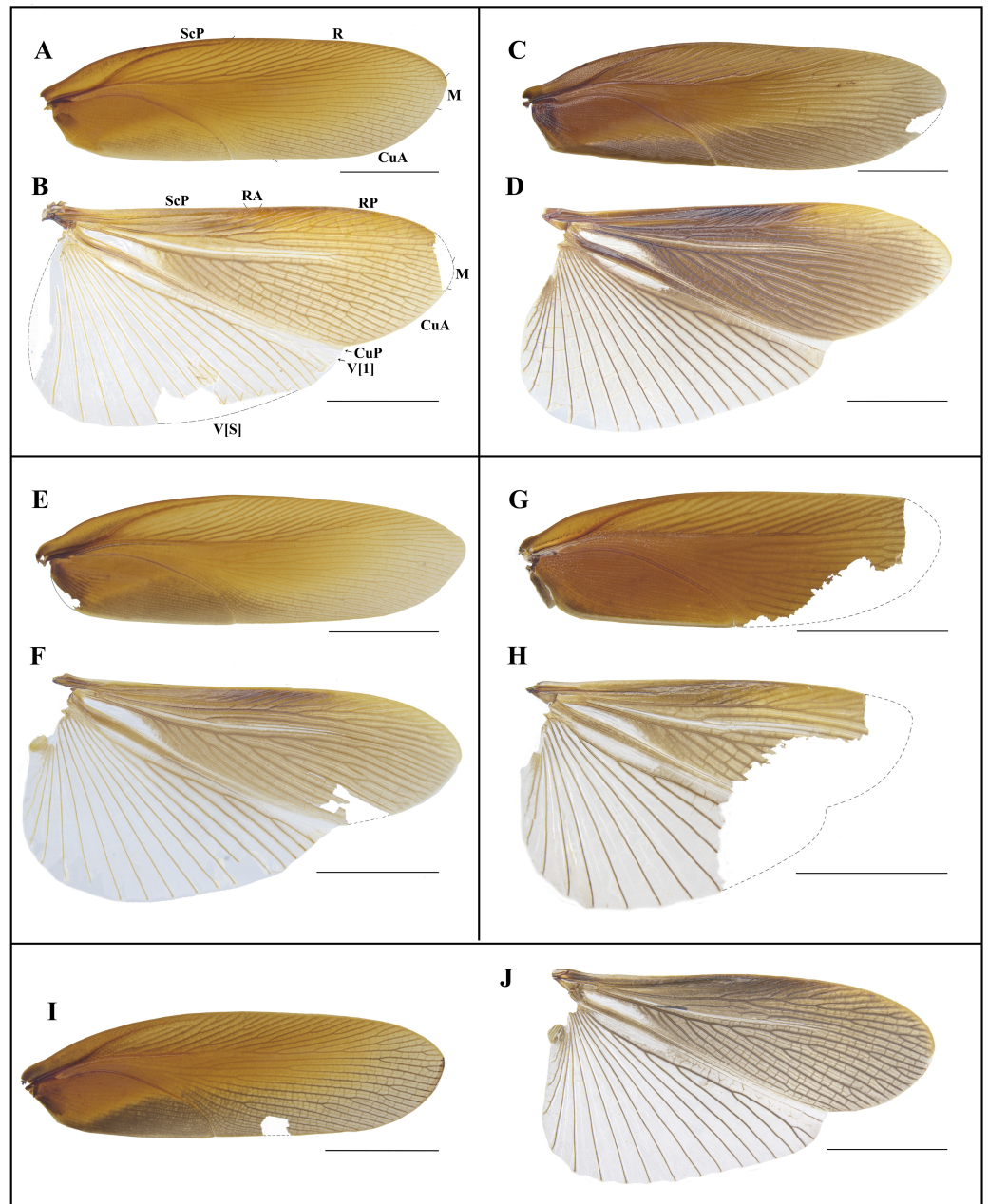
Figure 7 Photographs of tegmen and hind wings of *Homalosilpha*. (A–B) *H. obtusangula* sp. nov. (C–D) *H. recta* sp. nov.; (E–F) *H. alba* sp. nov. (G–H) *Homalosilpha* sp. (I–J) *H. clavellata* sp. nov. Scale bars = 10 mm.

sharp and protruded outward; subgenital plate of male asymmetrical, left hind corner angled while right hind corner round, styli similar (Figs. 8G and 8H).

Male genitalia: Left phallomere: L1 lamellar; margin of L2d with small spines, posterior of L2v produced with a spiny projection to the end; L3 with a spiny projection, the basal broad, tapering down, the terminus bifurcate, the lengths equal (Fig. 8I). Right phallomere:
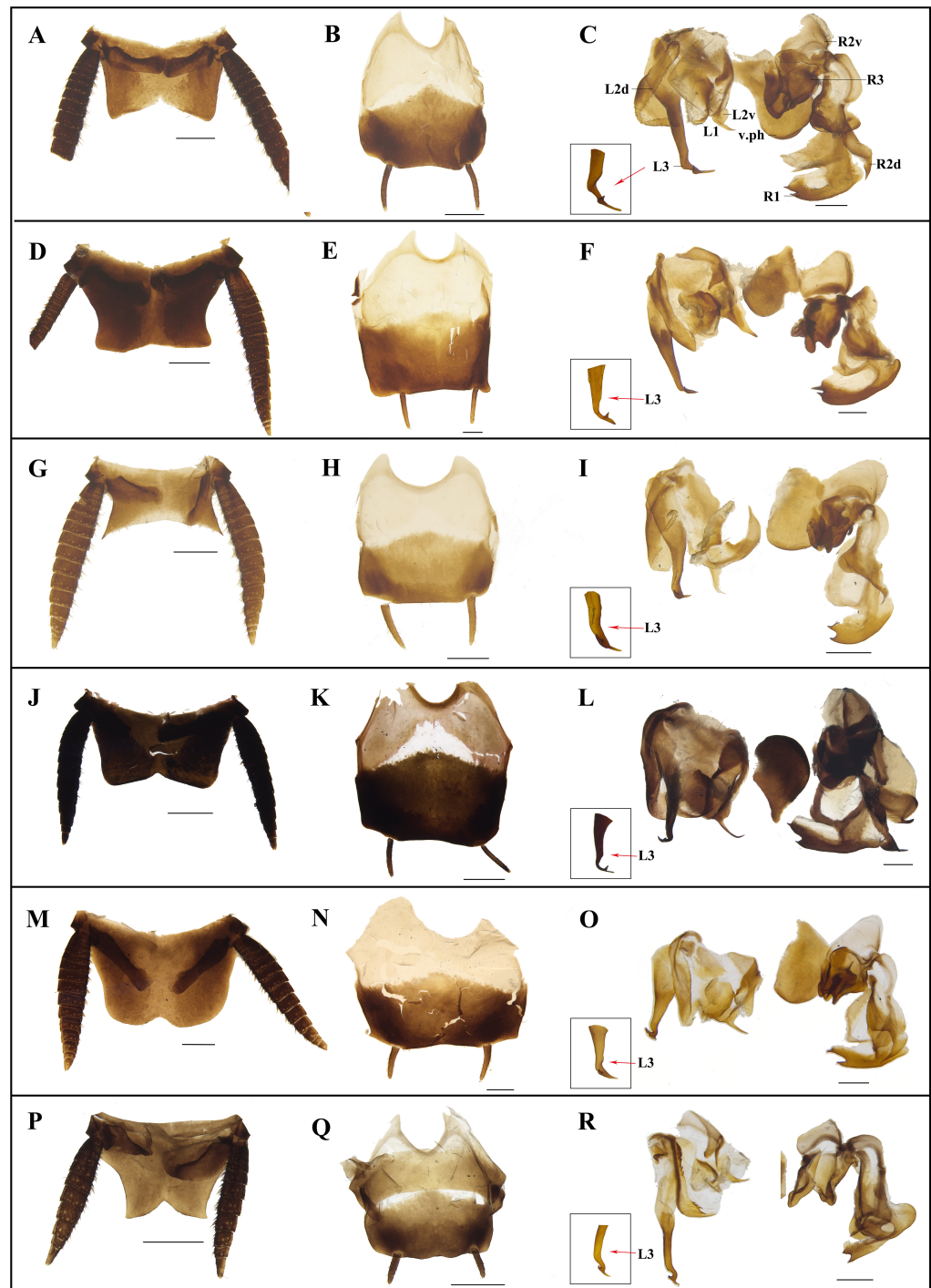
Figure 8 Photographs of male genitalia of *Homalosilpha* and *Mimosilpha* species. (A–C) *H. obtusangula* sp. nov., holotype. (D–F) *H. recta* sp. nov., holotype. (G–I) *H. alba* sp. nov., holotype. (J–L) *H. clavellata* sp. nov., holotype. (M–O) *H. kryzhanovskii*. (P–R) *M. disticha*. A, D, G, J, M, P, supra-anal plate, dorsal view; B, E, H, K, N, Q, subgenital plate, ventral view; C, F, I, L, O, R, phallomere, dorsal view. Scale bars = 1 mm.

Figure 9 **Habitats of *Homalosilpha*. and *Mimosilpha* species from China.** (A) *M. disticha* found on lichenous and mossy tree trunk (Dadugang, Jinghong, Yunnan). (B) *H. kryzhanovskii* found under the bark (Dadugang, Jinghong, Yunnan). (C) Nymphs of *M. distincta,* one was eating a dipteran insect (Dadugang, Jinghong, Yunnan). (D) A female *Homalosilpha* sp. (Mt. Ailaoshan, Yunnan). (E) A nymph of *Homalosilpha* species from Mengla, Xishuangbanna, Yunan (collected by Jianyue Qiu and Hao Xu). (A–C) photographed by Xinran Li. (D–F) photographed by Lu Qiu.

R1 foot-shaped, left margin with two equal spines; terminal of R2d unciform, R2v fold sclerite; R3 with complicated and broad sclerite (Fig. 8I).

Remarks. *H. alba* is similar to *H. kryzhanovskii* (Figs. 6I–6L, 8M–8O) but can be distinguished from *H. kryzhanovskii* by the following characters: (1) the black spots smaller

Table 1 Primers used in this study.

Genes	Forward/ Reverse	Sequences (5′-3′)	References
12S	F	ATCTATGTTACGACTTAT	*Inward, Beccaloni & Eggleton (2007)*
	R	AAACTAGGATTAGATACCC	*Kambhampati (1995)*
16S	F	CGCCTGTTTAACAAAAACAT	*Simon et al. (1994)*
	R	CGCCTGTTTAACAAAAACAT	*Cognato & Vogler (2001)*
18S	F	CTGGTTGATCCTGCCAGT	*Hillis & Dixon (1991)*
	R	TAATGATCCTTCCGCAGGTTCACCT	*Halanych, Lutz & Vrijenhoek (1998)*
28S	F	ACACGGACCAAGGAGTCTAAC	*Inward, Beccaloni & Eggleton (2007)*
	R	GTCCTGCTGTCTTAAGCAACC	
COII	F	AGAGCWTCACCTATTATAGAAC	*Park et al. (2004)*
	R	GTARWACRTCTGCTGCTGTTAC	
H3	F	ATGGCTCGTACCAAGCAGACVGC	*Inward, Beccaloni & Eggleton (2007)*
	R	ATATCCTTRGGCATRATRGTGAC	
COI	F	GGTCAACAAATCATAAGATATTGG	*Folmer et al. (1994)*
	R	TAAACTTCAGGGTGACCAAAAAATCA	

Homalosilpha clavellata Liao et Che sp. nov.
(Figs. 6A–6H, 7G and 7H, 8J–8L)
urn:lsid:zoobank.org:act:944DAC55-EAA7-4FB5-955B-5D5EBE3E7654

and thinner than *H. kryzhanovskii* in pronotum; and (2) the lateral angles of supra-anal plate sharp, however in *H. kryzhanovskii* nearly round.

Holotype. CHINA: Yunnan: male (SWUB128-H), Tongbiguan Township, Yingjiang County, 1130 m, 2018.IV.30, Lu Qiu & Wenbo Deng leg.

Paratype. 1 female (SWUB128-P1), CHINA: Yunnan: Tongbiguan Township, Yingjiang County, 1130 m, 2018.IV.30, Lu Qiu & Wenbo Deng leg.

Etymology. This species epithet is derived from the Latin word '*clavellatus*' referring to the terminal of R2d being produced in a stick shape.

Description. Male. Body length 22.8 mm; overall length including tegmina 29.0 mm; pronotum length × width 4.4 × 7.1 mm. Female. Body length 23.2 mm; overall length including tegmina 29.3 mm; pronotum length × width 5.5 × 8.1 mm.

Coloration: body generally black. Interocular space with a white transverse band, distal half of clypeus white. Pronotum white, margins black outlined; center of the pronotum with symmetrical blackish markings (Figs. 6A and 6B). Tegmen reddish brown, wings hyaline, blackish brown except the anal area (Figs. 7G and 7H). Tibiae and tarsi reddish brown (Fig. 6B).

Head with vertex unsheltered by pronotum. Interocular distance slightly narrower than the distance between antennae sockets. Pronotum nearly hexagonal, broadest on the basal half but near the middle, the anterior pattern connected with lateral pattern, the lateral pattern bold, the vertical pattern connected with posterior pattern, the posterior band bold and with two spots on the band (since the pronotum of the holotype male is deformed, thus

Liao et al. (2021), *PeerJ*, DOI 10.7717/peerj.10618

Table 2 Pairwise genetic divergence and the variance of the underlying distribution of distances calculated by using K2P model and bootstrap method respectively using cytochrome oxidase subunit I (*COI*) gene sequences in MEGA.

Species	Accession number	1	2	3	4	5	6	7	8	9	10	11	12
Homalosilpha cf. *javanica*	MW201581												
Homalosilpha cf. *javanica*	MW201582	0.000											
Homalosilpha nigricans	MW201583	0.036	0.036										
Homalosilpha clavellata sp. nov.	MW201584	0.044	0.044	0.039									
Homalosilpha clavellata sp. nov.	MW201585	0.044	0.044	0.039	0.000								
Homalosilpha sp.	MW201586	0.054	0.054	0.047	0.031	0.031							
Homalosilpha kryzhanovskii	MW201587	0.051	0.051	0.046	0.035	0.035	0.056						
Homalosilpha arcifera	MW201588	0.079	0.079	0.084	0.072	0.072	0.083	0.084					
Homalosilpha alba sp. nov.	MW201590	0.070	0.070	0.081	0.064	0.064	0.079	0.077	0.047				
Homalosilpha alba sp. nov.	MW201591	0.072	0.072	0.082	0.065	0.065	0.081	0.079	0.049	0.002			
Mimosilpha disticha	MW201592	0.081	0.081	0.077	0.074	0.074	0.079	0.084	0.075	0.075	0.077		
Mimosilpha disticha	MW201593	0.081	0.081	0.077	0.074	0.074	0.079	0.084	0.075	0.075	0.077	0.000	
Mimosilpha disticha	MW201594	0.077	0.077	0.077	0.069	0.069	0.077	0.081	0.070	0.074	0.075	0.006	0.006

this description is only based on the female paratype) (Figs. 6A–6H). Male supra-anal plate broad and symmetrical, nearly trapezoidal, but with a shallow, obtuse-angled invagination at the center of hind margin; male subgenital plate asymmetrical, left hind corner more protruded than that of the right, styli similar, thin (Figs. 8J and 8K).

Male genitalia: Left phallomere: L1 broad and lamellar; margin of L2d with small and dense spines, posterior of L2v produced as an acerose spiny projection to the end; L3 with a spiny projection, the basal broad, tapering down, the terminal bifurcate (Fig. 8L). Right phallomere: R1 foot-shaped, posterior with two spines; terminal of R2d clubbed, R2v fold sclerite and the end with a spine; R3 with broad sclerite (Fig. 8L).

Remarks. *H . clavellata* sp. nov. is similar to *H. arcifera*, but can be distinguished by the following characters: (1) different irregular maculae on the pronotum, large in *H. clavellata* sp. nov., while *H. arcifera*, small; (2) face and body black in *H. clavellata* sp. nov., while in *H. arcifera*, yellowish white. Besides, the pronotum of the male holotype is deformed with posterior and anterior margins deeply concave. We utilized DNA barcoding to pair this species, and the genetic distance between them was 0.00%.

Homalosilpha sp.
(Figs. 5M–5P, 7I–7J)

Material examined. 2 females (SWUB129-1, SWUB129-2), CHINA: Yunnan: Yaonan Village, Mt Ailao, Xinping County, 2018.V.24, Lu Qiu & Zhiwei Dong leg.

Description. Female. Body length 22.8–23.5 mm; overall length including tegmen 29.0–30.2 mm; pronotum length × width 4.4–5.0 × 6.9–7.1 mm.

Coloration: Body generally black. Interocular space with a white transverse band. Pronotum white, margins with black outline, hind margin black; center of the pronotum with symmetrical blackish markings. Tegmina brown, wings hyaline. Abdomen brown. Tibiae and tarsi yellow brown.

Head with vertex unsheltered by pronotum. Interocular distance slightly narrower than the distance between antennae sockets. Pronotum nearly hexagonal, broadest near the middle; the anterior pattern polygonal, the lateral pattern with two patterns, the central pattern connected with vertical pattern, the vertical pattern bold and the posterior bifurcated, the posterior band bold. Supra-anal plate broad, symmetrical and with ridges, cerci with obvious segmentation. Subgenital plate symmetrical, divided in two valves.

Natural History. Individuals were captured during night on the village roads (Lu Qiu, personal observation).

Mimosilpha Bey-Bienko, 1957
Mimosilpha Bey-Bienko, 1957: 905. Type species: *Mimosilpha disticha Bey-Bienko, 1957 Princis, 1966b*: 459.

Diagnosis. Body small. The diagnoses are similar to *Homalosilpha* except the outer edge of middle and hind tibiae with two rows of spines (Fig. 4) and the margin of L2d with bigger serration (Fig. 8).

Mimosilpha disticha *Bey-Bienko, 1957*
(Figs. 6M–6P, 8P–8R)
Mimosilpha disticha *Bey-Bienko, 1957*: 905; *Princis, 1966b*: 459

Material examined. 11 males, 7 females (SWUB130-1, SWUB130-2…SWUB130-17, SWU130-18), CHINA: Yunnan: Dadugang, Jinghong City, Xishuangbanna, 2014.IV.28-29, Xinran Li & Hongguang Liu leg; 1 male (SWU130B-19), CHINA: Yunnan: Jinghong City, Xishuangbanna, 545 m, 1974.V.14-15, Io Chou & Feng Yuan leg.

Redescription. Male. Body length 18.2–20.5 mm; overall length including tegmen 22.6–24.9 mm; pronotum length × width 3.7–4.6× 5.4–6.3 mm. Female. Body length 19.2–22.4 mm; overall length including tegmen 21.3–25.7 mm; pronotum length × width 4.3–4.7 × 5.7–6.5 mm.

Coloration. Similar in both sexes. Body dark brown (Figs. 6M and 6N). Pronotum white, with a large central black spot on middle disk, margins with black outline, hind margin black (Figs. 6O and 6P). Tegmen dark brown, wing hyaline, brown except the anal area. Abdomen brown to dark brown. Tibiae and tarsi brown (Fig. 6N).

Head with vertex unsheltered by pronotum. Interocular distance narrower than the distance between antennae sockets. Pronotum nearly hexagonal, broadest near the middle, large black spot connected to the hind margin. Legs with sparse spines. Supra-anal plate of male broad and symmetrical, nearly trapezoidal, posterior margin widely concave, the lateral margin concave, both lateral hind angles sharp; male subgenital plate asymmetrical, left hind corner round, hind margin wavy (Figs. 8P and 8Q).

Male genitalia: Left phallomere: L1, L2 and L3. L1 lamellar; margin of L2d with small spines, posterior of L2v produced a spiny projection to the end; L3 with a spiny projection, the basal broad, tapering down, the terminal bifurcated (Fig. 8R). Right phallomere: R1, R2 and R3. R1 foot-shaped, posterior with two spines; terminal of R2d unciform, R2v fold sclerite; R3 simple and broad (Fig. 8R).

DISCUSSION

Due to the similar pattern bearing in the pronotum by some *Homalosilpha* species (*Bey-Bienko, 1969*), i.e., *H. arcifera*, *H. javanica*, *H. kryzhanovskii*, *H. ustulata*, *H. valida*, *H. alba* sp. nov., *H. recta* sp. nov., it is very challenging to distinguish them based only on morphological data. Fortunately, our results show that DNA-based species delimitation methods perform well for *Homalosilpha* species, and also did well in matching male and female. Therefore, *COI* can be recommended as a single DNA barcode for *Homalosilpha*.

Homalosilpha is closely related to *Mimosilpha* not only in appearance but also in phylogenetic analysis. Apart from the slight difference in body size (*Homalosilpha*: medium to large, *Mimosilpha*: small), the diagnostic character given by *Bey-Bienko (1957)* to separate *Mimosilpha* and *Homalosilpha* was the number of rows of spines existing in the edge of hind tibiae (*Homalosilpha*: 3, *Mimosilpha*: 2). ML and BI analyses showed that *Homalosilpha* and *Mimosilpha* were monophyletic groups. *Homalosilpha* was recovered as the sister group of *Mimosilpha*.

Periplaneta americana, whose tibiae are also ornamented with strong spines, usually depend on their spines to brace themselves against the sides of a burrow and provide a stable platform for the transmission of force (*Bell, Nalepa & Roth, 2007*). Sometimes spines at the tip of tibiae will assist the tarsal claws to climb rough surfaces (*Bell, Nalepa & Roth, 2007*). It can be inferred that the spines on the tibiae of *Mimosilpha* and *Homalosilpha* also play a certain role in the process of movement. According to information observed so far (25 specimens of *Homalosilpha* and 25 specimens of *Mimosilpha*, including 12 *Homalosilpha* species from original description), we inferred the number of rows of spines to be stable in different individuals and even in nymphs. In field collection, one *H. kryzhanovskii* was found on wooden poles and two *Homalosilpha* sp. were found on the road, but more *Mimosilpha disticha* were found on tree trunks covered with lichen and moss (Li XR, pers. obs., 2014) (Fig. 9). We speculate that different rows of spines exhibited by *Mimosilpha* and *Homalosilpha* on the edge of hind tibiae might reflect adaptation to different habitats. So we do not treat *Mimosilpha* as the junior synonym of *Homalosilpha* although only minor morphological differences exist between them. We will explore more evidence concerning this relationship later.

Although our data are insufficient, the ML and BI phylogenetic analyses also reflected that Polyzosteriinae, Archiblattinae and Blattinae are paraphyletic with high support values. At the beginning, some scholars proposed that *Archiblatta* should be placed in Blattinae because of the valvular structure of the female subgenital plate (*Shelford, 1910*; *Bruijning, 1948*); but *Roth (2003)* still recognized Archiblattinae as a subfamily because of the absence or greatly reduced femoral armament. *Murienne (2009)* concatenated *12S* and *H3* to construct ML and BI, and the results revealed Archiblattinae (*Archiblatta*) and Blattinae form a monophyletic group. However, *Djernæs, Klass & Eggleton (2015)* proposed that Polyzosteriinae (*Drymaplaneta*, *Eurycotis*), Archiblattinae (*Archiblatta*) and Blattinae (*Periplaneta*, *Deropeltis*) might be artificial and not natural groups based on a phylogenetic tree combining 8 genes (*12S*, *16S*, *18S*, *tRNA-Leu*, *COII*, *tRNA-Lys*, *H3*). *Bourguignon et al. (2018)* also discovered Archiblattinae (*Protagonisa*) and Blattinae are paraphyletic via mitochondrial phylogeny. As these issues are reflected by our results, the monophyly of Polyzosteriinae, Archiblattinae and Blattinae should be questioned and more attention paid to solving this dilemma. Therefore, additional sampling of Archiblattinae and Blattinae will help improve our understanding of Blattidae in the future.

CONCLUSION

Our study shows that molecular methods based on COI data delimit MOTUs for *Homalosilpha* that are highly consistent with those based on morphological characters. Therefore, COI is recommended as an effective DNA Barcode for *Homalosilpha*. Our phylogeny based on mitochondrial and nuclear genes reveals the close relationship of *Homalosilpha* and *Mimosilpha*, but the introduction of more samples is therefore recommended to better improve our understanding of those highly similar genera. Although limited samples of Blattidae are included in our study, the paraphyly of Polyzosteriinae, Archiblattinae and Blattinae is found with high support values and

our study will pave the way for a better understanding of the relationship among those subfamilies.

Terminology abbreviations

L1, L2, L3	sclerites of the left phallomere
L2d/R2d	L2/R2 dorsal
R1, R2, R3	sclerites of the right phallomere
L2v/R2v	L2/R2 ventral
v.ph	ventral phallomere
CuA	cubitus anterior
CuP	cubitus posterior
RP	radius posterior
ScP	subcosta posterior
Pcu	postcubitus
M	media
R	radius
RA	radius anterior
V	vannal veins

ACKNOWLEDGEMENTS

We thank all collectors in this paper for their efforts in collecting specimens. We also would like to thank John Richard Schrock for proofreading the English.

Funding

This work was supported by the National Natural Science Foundation of China (Nos. 31772506, 31872271) and a Program of the Ministry of Science and Technology of the People's Republic of China (2015FY210300). The funders had no role in study design, data collection and analysis, decision to publish, or preparation of the manuscript.

Grant Disclosures

The following grant information was disclosed by the authors:
National Natural Science Foundation of China: 31772506, 31872271.
Program of the Ministry of Science and Technology of the People's Republic of China: 2015FY210300.

Competing Interests

The authors declare there are no competing interests.

Author Contributions

- Shuran Liao conceived and designed the experiments, performed the experiments, analyzed the data, prepared figures and/or tables, authored or reviewed drafts of the paper, and approved the final draft.
- Yishu Wang, Duting Jin and Rong Chen performed the experiments, prepared figures and/or tables, and approved the final draft.
- Zongqing Wang conceived and designed the experiments, authored or reviewed drafts of the paper, and approved the final draft.
- Yanli Che conceived and designed the experiments, analyzed the data, authored or reviewed drafts of the paper, and approved the final draft.

Data Availability

12S data are available at GenBank: MW218556 to MW218567.

16S data are available at GenBank: MW218581 to MW218592

18S data are available GenBank: MW218568 to MW218578

28S data are available GenBank: MW218593 to MW218604

COII data are available GenBank: MW201821 to MW201830

H3 data are available GenBank: MW201809 to MW201820

COI data are available GenBank: MW201581 to MW201594

The other GenBank accession numbers were recorded in Tables S1 and S2.

All specimens were kept in College of Plant Protection, Southwest University, and their accession numbers as follows:

Homalosilpha obtusangula Liao et Che sp. nov.: SWUB125-H, SWUB125-P1

Homalosilpha recta Liao et Che sp. nov.: SWUB126-H

Homalosilpha alba Liao et Che sp. nov.: SWUB127-H, SWUB127-P1, SWUB127-P2, SWU B127-P3

Homalosilpha clavellata Liao et Che sp. nov.: SWUB128-H, SWUB128-P1

Homalosilpha sp.: SWUB129-1, SWUB129-2

Mimosilpha disticha BeyBienko1957: SWUB130-1, SWUB130-2 - SWUB130-17, SWU130-18, SWU130B-19

New Species Registration

The following information was supplied regarding the registration of a newly described species:

Publication LSID: urn:lsid:zoobank.org:pub:74F6BF88-9FFD-40DB-9C8B-D7650491F0EE

Homalosilpha clavellata sp. nov. LSID: urn:lsid:zoobank.org:act:944DAC55-EAA7-4FB5-955B-5D5EBE3E7654

Homalosilpha obtusangula sp. nov. LSID: urn:lsid:zoobank.org:act:8713E5A8-D25B-4DFB-9E44-3B1E719AE2FC

Homalosilpha recta sp. nov. LSID: urn:lsid:zoobank.org:act:88B30874-14A8-4035-B200-262CF60E09D6

Homalosilpha alba sp.nov. LSID: urn:lsid:zoobank.org:act:ED3EEF8E-FD76-47F7-AA5A-ABE9F3CA6724.

Supplemental Information

Supplemental information for this article can be found online at http://dx.doi.org/10.7717/peerj.10618#supplemental-information.

REFERENCES

Beccaloni GW. 2014. Cockroach species file online. Version 5.0/5.0. World Wide Web electronic publication. *Available at http://Cockroach.SpeciesFile.org* (accessed on 18 December 2019).

Bell WJ, Nalepa CA, Roth LM. 2007. *Cockroaches: ecology, behavior, and natural history*. The Johns Hopkins University Press.

Bey-Bienko GY. 1957. Blattoidea of Szechuan and Yunnan. *Communication I. Entomologicheskoe Obozrenie* **36**:895–915.

Bey-Bienko GY. 1969. New genera and species of cockroaches (Blattoptera) from tropical and subtropical Asia. *Entomologica Review* **48**:528–548 DOI 10.1016/j.sbspro.2015.07.500.

Bourguignon T, Tang Q, Ho SYW, Juna F, Wang ZQ, Arab DA, Cameron SL, Walker J, Rentz D, Evans TA, Lo N. 2018. Transoceanic dispersal and plate tectonics shaped global cockroach distributions: evidence from mitochondrial phylogenomics. *Molecular Biology and Evolution* **35**:970–983 DOI 10.1093/molbev/msy013.

Bruijning CFA. 1948. Studies on Malayan Blattidae. *Zoologische Mededelingen* **29**:1–174.

Brunner von Wattenwyl C. 1865. *Nouveau Système des Blattaires*. Vienna: G-Braumüller, 1–426.

Burmeister H. 1838. *Handbouch der Entomologie*. Berlin: Reimer, 397–756.

Che YL, Gui SH, Lo N, Ritchie A, Wang ZQ. 2017. Species delimitation and phylogenetic relationships in Ectobiid cockroaches (Dictyoptera, Blattodea) from China. *PLOS ONE* **12(1)**:e0169006 DOI 10.1371/journal.pone.0169006.

Cognato AI, Vogler AP. 2001. Exploring data interaction and nucleotide alignment in a multiple gene analysis of *Ips* (Coleoptera: Scolytinae). *Systematic Biology* **50**:758–780 DOI 10.1080/106351501753462803.

Djernæs M. 2018. Biodiversity of Blattodea—the cockroaches and termites: science and society. *Insect Biodiversity* **2**:359–387 DOI 10.1002/9781118945582.ch14.

Djernæs M, Klass KD, Eggleton P. 2015. Identifying possible sister groups of Cryptocercidae+Isoptera: a combined molecular and morphological phylogeny of Dictyoptera. *Molecular Phylogenetics and Evolution* **84**:284–303 DOI 10.1016/j.ympev.2014.08.019.

Evangelista DA, Buss L, Ware JL. 2013. Using DNA barcodes to confirm the presence of a new invasive cockroach pest in New York City. *Journal of Economic Entomology* **106**:2275–2279 DOI 10.1603/EC13402.

Evangelista DA, Wipfler B, Béthoux O, Donath A, Fujita M, Kohli KM, Legendre F, Liu SL, Machida R, Misof B, Peters RS, Podsiadlowski L, Rust J, Schuette K, Tollenaar W, Ware JL, Wappler T, Zhou X, Meusemann K, Simon S. 2019. An integrative phylogenomic approach illuminates the evolutionary history of cockroaches and

termites (Blattodea). *Proceedings of the Royal Society B: Biological Sciences* **286**:1–9 DOI 10.1098/rspb.2018.2076.

Folmer O, Black M, Hoeh W, Lutz R, Vrijenhoek RC. 1994. DNA primers for amplification of mitochondrial cytochrome c oxidase subunit I from diverse metazoan invertebrates. *Molecular Marine Biology and Biotechnology* **3**:294–299.

Halanych KM, Lutz RA, Vrijenhoek RC. 1998. Evolutionary origins and age of vestimentiferan tube–worms. *Cahiers De Biologie Marine* **39**:355–358 DOI 10.1515/botm.1998.41.1-6.113.

Hanitsch R. 1915. Malayan Blattidae. Part I. *Journal Straits Branch Royal Asiatic Society* **69**:17–178.

Hillis DM, Dixon MT. 1991. Ribosomal DNA: molecular evolution and phylogenetic inference. *The Quarterly Review of Biology* **66**:411–453 DOI 10.1086/417338.

Inward D, Beccaloni G, Eggleton P. 2007. Death of an order: a comprehensive molecular phylogenetic study confirms that termites are eusocial cockroaches. *Biology Letters* **3(3)**:331–335 DOI 10.1098/rsbl.2007.0102.

Kambhampati S. 1995. A phylogeny of cockroaches and related insects based on DNA sequence of mitochondrial ribosomal RNA genes. *Proceedings of the National Academy of Sciences of the United States of America* **92**:2017–2020 DOI 10.1073/pnas.92.6.2017.

Kimura M. 1980. A simple method for estimating evolutionary rates of base substitutions through comparative studies of nucleotide sequences. *Journal of Molecular Evolution* **16**:111–120 DOI 10.1007/bf01731581.

Kirby WF. 1904. A synonymic catalogue of orthoptera Vol. 1. *Orthoptera Euplexoptera Cursoria, et Gressoria* **18**:61–209.

Kumar R. 1975. A review of the cockroaches of West Africa and the Congo basin (Dictyoptera: Blattaria). *Bulletin de l'Institut fondamental d'Afrique noire (Sciences naturelles)* **37**:27–121.

Kumar S, Stecher G, Tamura K. 2016. MEGA7: molecular evolutionary genetics analysis version 7.0 for bigger datasets. *Molecular Biology and Evolution* **33**:1870–1874 DOI 10.1093/molbev/msw054.

Lanfear R, Calcott B, Ho SYW, Guindon S. 2012. PartitionFinder: combined selection of partitioning schemes and substitution models for phylogenetic analyses. *Molecular Biology and Evolution* **29**:1695–1701 DOI 10.1093/molbev/mss020.

Legendre F, Nel A, Svenson GJ, Robillard T, Pellens R, Grandcolas P. 2015. Phylogeny of Dictyoptera: dating the origin of cockroaches, praying mantises and termites with molecular data and controlled fossil evidence. *PLOS ONE* **10(7)**:e0130127 DOI 10.1371/journal.pone.0130127.

Li XR, Zheng YH, Wang CC, Wang ZQ. 2018. Old method not old-fashioned: parallelism between wing venation and wing-pad tracheation of cockroaches and a revision of terminology. *Zoomorphology* **137**:519–533 DOI 10.1007/s00435-018-0419-6.

Liao SR, Wang ZQ, Che YL. 2019. A new genus and a new species in the subfamily Polyzosteriinae (Blattodea, Blattidae) from China. *ZooKeys* **852**:85–100 DOI 10.3897/zookeys.852.33325.

McKittrick FA. 1964. Evolutionary studies of cockroaches. *Cornell University Agricultural Experiment Station Memoir* **389**:1–197.

Murienne J. 2009. Molecular data confirm family status for the tryonicus–lauraesilpha group (Insecta: Blattodea: Tryonicidae). *Organisms Diversity and Evolution* **9**:44–51 DOI 10.1016/j.ode.2008.10.005.

Park YC, Maekawa K, Matsumoto T, Santoni R, Choe JC. 2004. Molecular phylogeny and biogeography of the Korean woodroaches *Cryptocercus* spp. *Molecular Phylogenetics and Evolution* **30**:450–464 DOI 10.1016/S1055-7903(03)00220-3.

Princis K. 1966a. Kleine Beitrage zur Kenntnis der Blattarien und ihrer Verbreitung. IX. *Opuscula Entomologica* **31**:43–60.

Princis K. 1966b. Blattariae: Suborbo [sic] Blattoidea. Fam.: Blattidae, Nocticolidae. In: Beier M, ed. *Orthopterorum Catalogus. Pars 8.* ’s-Gravenhage (The Hague, Netherlands): Uitgeverij. Dr. W. Junk, 402–614.

Ronquist F, Teslenko M, Van der Mark P, Ayres DL, Darling A, Höhna S, Larget B, Liu L, Huelsenbeck JP. 2012. MrBayes 3.2: efficient Bayesian phylogenetic inference and model choice across a large model space. *Systematic Biology* **61**:539–542 DOI 10.1093/sysbio/sys029.

Roth LM. 1999. Descriptions of new taxa, redescriptions, and records of cockroaches, mostly from Malaysia and Indonesia (Dictyoptera: Blattaria). *Oriental Insects* **33**:109–185 DOI 10.1080/00305316.1999.10433789.

Roth LM. 2003. Systematics and phylogeny of cockroaches (Dictyoptera: Blattaria). *Oriental Insects* **37**:1–186 DOI 10.1080/00305316.2003.10417344.

Shelford R. 1908. New species of Blattidae in the collection of the Deutsche Entomologische National-Museum, (Orthoptera). *Deutsche Entomologische Zeitschrift* **1908**:115–131.

Shelford R. 1910. Orthoptera: Blattidae: Blattinae in P. Wytsman. *Genera Insectorum: fasc* **109**:1–27.

Simon C, Frati F, Beckenbach A, Crespi B, Liu H, Flook P. 1994. Evolution, weighting, and phylogenetic utility of mitochondrial gene sequences and a compilation of conserved polymerase chain reaction primers. *Annals of the Entomological Society of America* **87(6)**:651–701 DOI 10.1093/aesa/87.6.651.

Stål C. 1874. Recherches sur le système des Blattaires. *Bihang Till K. Svensk. Vet-Akad Handlingar* **2**:3–18.

Stamatakis A, Hoover P, Rougemont J. 2008. A rapid bootstrap algorithm for the RAxML web servers. *Systematic Biology* **57**:758–771 DOI 10.1080/10635150802429642.

Wang ZQ, Shi Y, Qiu ZW, Che YL, Lo N. 2017. Reconstructing the phylogeny of Blattodea: robust support for interfamilial relationships and major clades. *Scientific Reports* **7**:3903 DOI 10.1038/s41598-017-04243-1.

Ware JL, Litman J, Klass KD, Spearman LA. 2008. Relationships among the major lineages of Dictyoptera: the effect of outgroup selection on dictyopteran tree topology. *Systematic Entomology* **33**:429–450 DOI 10.1111/j.1365-3113.2008.00424.x.

Xia X. 2013. DAMBE 5: a comprehensive software package for data analysis in molecular biology and evolution. *Molecular Biology and Evolution* **30**:1720–1728 DOI 10.1093/molbev/mst064.